

RESEARCH

Open Access



# Mapping neural correlates of biological motion perception in autistic children using high-density diffuse optical tomography

Dalin Yang<sup>1†</sup>, Alexandra M. Svoboda<sup>1†</sup>, Tessa G. George<sup>1</sup>, Patricia K. Mansfield<sup>1,2</sup>, Muriah D. Wheelock<sup>1,3,4</sup>, Mariel L. Schroeder<sup>1,5</sup>, Sean M. Rafferty<sup>1</sup>, Arefeh Sherafati<sup>1,6,7</sup>, Kalyan Tripathy<sup>1,4,8</sup>, Tracy Burns-Yocum<sup>1,9</sup>, Elizabeth Forsen<sup>1,10</sup>, John R. Pruett<sup>11</sup>, Natasha M. Marrus<sup>11</sup>, Joseph P. Culver<sup>1,3,4,6,12,13</sup>, John N. Constantino<sup>11,14,15</sup> and Adam T. Eggebrecht<sup>1,3,4,6,12,13\*</sup>

## Abstract

**Background** Autism spectrum disorder (ASD), a neurodevelopmental disorder defined by social communication deficits plus repetitive behaviors and restricted interests, currently affects 1/36 children in the general population. Recent advances in functional brain imaging show promise to provide useful biomarkers of ASD diagnostic likelihood, behavioral trait severity, and even response to therapeutic intervention. However, current gold-standard neuroimaging methods (e.g., functional magnetic resonance imaging, fMRI) are limited in naturalistic studies of brain function underlying ASD-associated behaviors due to the constrained imaging environment. Compared to fMRI, high-density diffuse optical tomography (HD-DOT), a non-invasive and minimally constraining optical neuroimaging modality, can overcome these limitations. Herein, we aimed to establish HD-DOT to evaluate brain function in autistic and non-autistic school-age children as they performed a biological motion perception task previously shown to yield results related to both ASD diagnosis and behavioral traits.

**Methods** We used HD-DOT to image brain function in 46 ASD school-age participants and 49 non-autistic individuals (NAI) as they viewed dynamic point-light displays of coherent biological and scrambled motion. We assessed group-level cortical brain function with statistical parametric mapping. Additionally, we tested for brain-behavior associations with dimensional metrics of autism traits, as measured with the Social Responsiveness Scale-2, with hierarchical regression models.

**Results** We found that NAI participants presented stronger brain activity contrast (coherent > scrambled) than ASD children in cortical regions related to visual, motor, and social processing. Additionally, regression models revealed multiple cortical regions in autistic participants where brain function is significantly associated with dimensional measures of ASD traits.

<sup>†</sup>Dalin Yang and Alexandra M. Svoboda are co-lead authors.

\*Correspondence:  
Adam T. Eggebrecht  
aeggebre@wustl.edu

Full list of author information is available at the end of the article



© The Author(s) 2024. **Open Access** This article is licensed under a Creative Commons Attribution-NonCommercial-NoDerivatives 4.0 International License, which permits any non-commercial use, sharing, distribution and reproduction in any medium or format, as long as you give appropriate credit to the original author(s) and the source, provide a link to the Creative Commons licence, and indicate if you modified the licensed material. You do not have permission under this licence to share adapted material derived from this article or parts of it. The images or other third party material in this article are included in the article's Creative Commons licence, unless indicated otherwise in a credit line to the material. If material is not included in the article's Creative Commons licence and your intended use is not permitted by statutory regulation or exceeds the permitted use, you will need to obtain permission directly from the copyright holder. To view a copy of this licence, visit <http://creativecommons.org/licenses/by-nc-nd/4.0/>.

**Limitations** Optical imaging methods are limited in depth sensitivity and so cannot measure brain activity within deep subcortical regions. However, the field of view of this HD-DOT system includes multiple brain regions previously implicated in both task-based and task-free studies on autism.

**Conclusions** This study demonstrates that HD-DOT is sensitive to brain function that both differentiates between NAI and ASD groups and correlates with dimensional measures of ASD traits. These findings establish HD-DOT as an effective tool for investigating brain function in autistic and non-autistic children. Moreover, this study established neural correlates related to biological motion perception and its association with dimensional measures of ASD traits.

**Keywords** Autism spectrum disorder, Neuroimaging, High-density diffuse optical tomography, Biological motion, Social perception

## Introduction

Autism spectrum disorder (ASD), a neurodevelopmental disorder impacting 1 in 36 children in the United States, is characterized by social communication deficits and restricted, repetitive patterns of behavior and interests [1, 2]. Autism is observed across all groups, regardless of race, ethnicity, and socio-economic status [3, 4], with a growing prevalence in recent years [3, 5, 6]. Although early signs of ASD may begin to appear by age six months, reliable individually predictive diagnostic indicators during the first year of life have yet to be established, and the median age at diagnosis is 49 months in the US [2, 7]. Early autism identification and a deeper understanding of the physiological mechanisms contributing to ASD will inform early interventions that may reduce impairments, enhance social skills development, increase independence, and improve academic success [8–10]. Brain-based biomarkers identified through functional magnetic resonance imaging (fMRI) may point to region-specific and network-level mechanisms that underlie behavioral variation in autism and may facilitate clinical subtyping, early diagnosis, and track response to interventions [9, 10]. However, the MRI environment can prove intolerable for many children due to noise, claustrophobia, and the need to lie supine and still [11]. Optical functional neuroimaging methods (e.g., functional near-infrared spectroscopy; fNIRS) are a potential solution to providing a more naturalistic functional neuroimaging environment amenable to studies on autistic children [12, 13]. Recent developments in high-density diffuse optical tomography (HD-DOT) methods have dramatically improved reliability and image quality over traditional fNIRS [14, 15], enabling functional neuroimaging with fMRI-comparable image quality in an open setting [14, 16, 17]. The utility of HD-DOT has been previously established in multiple groups including healthy adults [15, 16, 18–20], adults with Parkinson's Disease [15], adults with cochlear implants [21], school-age children [22, 23], and infants, including within clinical settings [24, 25]. Given the opportunity HD-DOT has to advance autism research, herein, we use HD-DOT to investigate brain function underlying passive viewing of

biological motion. This is the first study to establish its feasibility in a school-age autism cohort using a passive biological motion perception task. We specifically chose the biological motion task due to its common use in fMRI and eye tracking studies on ASD throughout childhood development [26–31].

Biological motion perception (BMP) is an evolutionarily conserved process [32–35] that plays a crucial role in filial attachment, predator detection, and social development [36, 37], whose difference has been implicated in ASD [9, 26]. While typically developing infants display a strong preference for viewing coherent point-light displays of biological motion over scrambled or inverted point-light displays [38, 39]—a preference that emerges rapidly over the first two years of life [38]—infants and toddlers who later receive an ASD diagnosis often do not exhibit this preference [9, 40, 41]. Increasing extant evidence supports the cascading effect of difference in BMP throughout childhood development as possible precursors for heterogeneous presentations of social communication associated with ASD [36, 40, 42]. Direct measures of the brain function underlying BMP may provide quantitative biomarkers for ASD that support both diagnostic and transdiagnostic analyses against quantitative behavioral, neurological, and genomic data, and bridge the gap between observable behaviors and underlying neurophysiological mechanisms [43–47].

Neuroimaging studies using task-based fMRI have demonstrated sensitivity to brain activity patterns that may inform ASD diagnosis using BMP stimuli [27, 43, 48, 49]. For example, Kaiser et al. (2010), a foundational study on brain function underlying BMP in children with autism, showed that the constellation of activity within 12 cortical regions was different for autistic children, non-autistic individuals (NAI) participants, and proband siblings (PS). This suggested that the brain function underlying BMP is related to the genetic background for ASD, which has been shown to be highly heritable [26, 50]. Additionally, a meta-analysis of eight fMRI studies on BMP summarized 62 foci and identified 6 clusters exhibiting stronger brain activity in NAI participants compared to the autistic cohort [42]. Conversely, other

fMRI studies using BMP stimuli have reported no significant group differences [48, 51]. The observed inconsistencies may stem from differences in experimental design, cohort (e.g., participant age range, autism symptom severity, cognitive capabilities), or motion artifacts [42]. Indeed, fMRI is limited in studies on naturalistic brain function in children because of the ergonomic constraints of the magnet bore and a sensitivity to motion-induced artifacts [52]. While optical methods like fNIRS and HD-DOT measure relative changes in a blood oxygenation level dependent signal akin to that of fMRI [53], they overcome the logistical limitations of fMRI and present a potential solution to provide a more naturalistic neuroimaging environment amenable to studies with autistic children throughout childhood development [12, 13, 54, 55].

Herein, we aimed to establish: (i) the feasibility of HD-DOT for evaluating brain function in children, (ii) the neural correlates of BMP, and (iii) the relationships between these neural correlates and dimensional behavioral autistic traits. To accomplish these aims, we used HD-DOT to evaluate brain responses of ASD, NAI, and PS school-age participants (age 7 to 18 years) as they passively viewed coherent and scrambled point-light displays of biological motion [26, 50, 56]. We assessed group-level cortical brain function with statistical parametric mapping. Additionally, we conducted an exploratory brain-wide investigation of how brain activity related to

dimensional autistic traits using hierarchical regression analyses with two complementary analyses. We hypothesized that: (i) HD-DOT is feasible for measuring brain function in autistic and non-autistic children; (ii) the brain contrast in response to coherent vs. scrambled biological motion will be stronger in the NAI than the ASD group; and (iii) the magnitude of this brain contrast will be negatively correlated with dimensional metrics of autistic traits.

**Methods**

**Participants**

Participants were recruited from the Washington University in St. Louis community and surrounding area. Written informed consent was obtained for each participant or guardian as approved by the Human Research Protection Office at Washington University School of Medicine. We recruited 112 participants age 7–18 years, including 46 individuals with a known diagnosis of ASD, 49 non-autistic individuals (NAI), and 17 proband siblings (PS) (Table 1). No participants had a documented history of neurological injury. The NAI participants had neither a suspected ASD diagnosis according to their parents/guardians nor any first-/second-degree relatives with confirmed or suspected autism. All participants in the ASD group had a community-ascertained ASD diagnosis based on the DSM-5. To confirm diagnosis and to measure autism severity along dimensions of social

**Table 1** Participant demographics and group characteristics

		ASD			NAI				
		Full sample (n=46)		Final sample (n=23)		Full sample (n=49)		Final sample (n=21)	
		Mean (SD)	n	Mean (SD)	n	Mean (SD)	n	Mean (SD)	n
Sex, Males: Females		33:13		19:4		30:19		12:9	
Age, years		13.1 (2.7)	46	14.6 (10.3)	23	12.2 (3.0)	49	13.1 (3.2)	21
SRS-2	Raw score	90.0 (29.2)	45	84.1 (26.5)	23	16.1 (12.3)	42	11.7 (9.6)	21
	T score	73.3 (12.6)	45	70.4 (10.9)	23	43.8 (5.0)	42	42.1 (4.1)	21
KBIT-2 IQ	Verbal	94.5 (19.2)	39	100.6 (14.1)	23	105.6 (9.8)	33	106.1 (9.8)	21
	Nonverbal	99.2 (17.7)	39	105.0 (10.3)	23	109.8 (13.8)	33	109.8 (13.0)	21
	Composite	96.3 (19.0)	40	103.4 (13.0)	23	109.3 (10.9)	33	109.4 (10.0)	21
ADOS Mod2	Overall	11.3 (2.9)	3	11.0 (0.0)	1				
	Social Com	8.3 (0.5)	3	8.0 (0.0)	1				
	RRB	3.0 (2.4)	3	3.0 (0.0)	1				
ADOS Mod3	Overall	15.4 (6.2)	13	14.2 (6.2)	9				
	Social Com	11.3 (5.7)	13	8.4 (4.8)	9				
	RRB	3.5 (2.7)	13	3.8 (2.6)	9				
ADOS Mod4	Overall	7.0 (2.9)	3	5.0 (1.0)	2				
	Social Com	8.4 (3.7)	5	8.0 (4.1)	4				
	RRB	1.4 (1.7)	5	1.8 (1.8)	4				
ADIR	Social	18.5 (5.6)	13	16.4 (5.6)	8				
	Verbal	12.8 (5.5)	13	11.0 (5.8)	8				
	RRB	4.2 (2.2)	13	3.8 (1.7)	8				

Standard deviation (SD), Number of sample (n). KBIT-2 IQ: Kaufmann Brief Intelligence Test, Second Edition, SRS-2: Social Responsiveness Scale, 2nd edition ADOS: Autism Diagnostic Observation Schedule, Social Com: Social Communication, RRB: Restricted, Repetitive Behaviors, ADI-R: Autism Diagnostic Interview – Revised

communication, restricted and repetitive behaviors, and adaptive functioning, participants in the ASD group were administered the Autism Diagnostic Observation Schedule (ADOS) and/or Autism Diagnostic Interview–Revised (ADI-R). All PS participants had a sibling with a community-ascertained autism diagnosis but did not have an autism diagnosis themselves.

**Behavioral measurements**

The Kaufmann Brief Intelligence Test (KBIT-2) provided three measures: verbal and nonverbal intelligence quotients (VIQ, NVIQ, respectively) and a composite intelligence quotient (IQ) [57]. The Social Responsiveness Scale, 2nd edition (SRS-2), provided a parent-reported measure of social reciprocity, with higher scores correspondent to higher levels of autism traits [58]. The SRS raw scores were converted to standardized SRS *t*-scores for analyses across a general population to avoid bias for age or sex. To control for variability due to significantly lower cognitive function, participants with standardized composite KBIT IQ < 70 were removed from analyses (five participants in the ASD group). To control for possible unknown variance, we excluded participants with missing IQ scores (16 NAI, 16 ASD, and 1 PS), and

missing SRS scores (2 NAI and 2 PS). Importantly, this data loss is attributed specifically to personnel factors due to ceasing data collection due to COVID-19 restrictions, and is not related to the task performance of the participants.

**HD-DOT System and data acquisition**

We used a previously described custom-built continuous wave HD-DOT system (Fig. 1A) [14, 15, 20]. The high-density array provided sensitivity in a field of view over approximately a third of the optically accessible cortex, including multiple cortical regions previously implicated in processing biological motion [26, 42]. The imaging cap supported multiple source-detector distances (i.e., first through fourth nearest neighbors defined as 13, 30, 39, and 47 mm), providing more than 1,200 spatially overlapping multi-distance measurements per wavelength that together deliver fMRI-comparable resolution via tomographic reconstruction at a frame rate of 10 Hz.

**Experimental procedure and stimuli**

Participants completed a 35-minute-long imaging session seated in an adjustable chair with a lumbar support pillow for comfort. The HD-DOT cap fit was guided

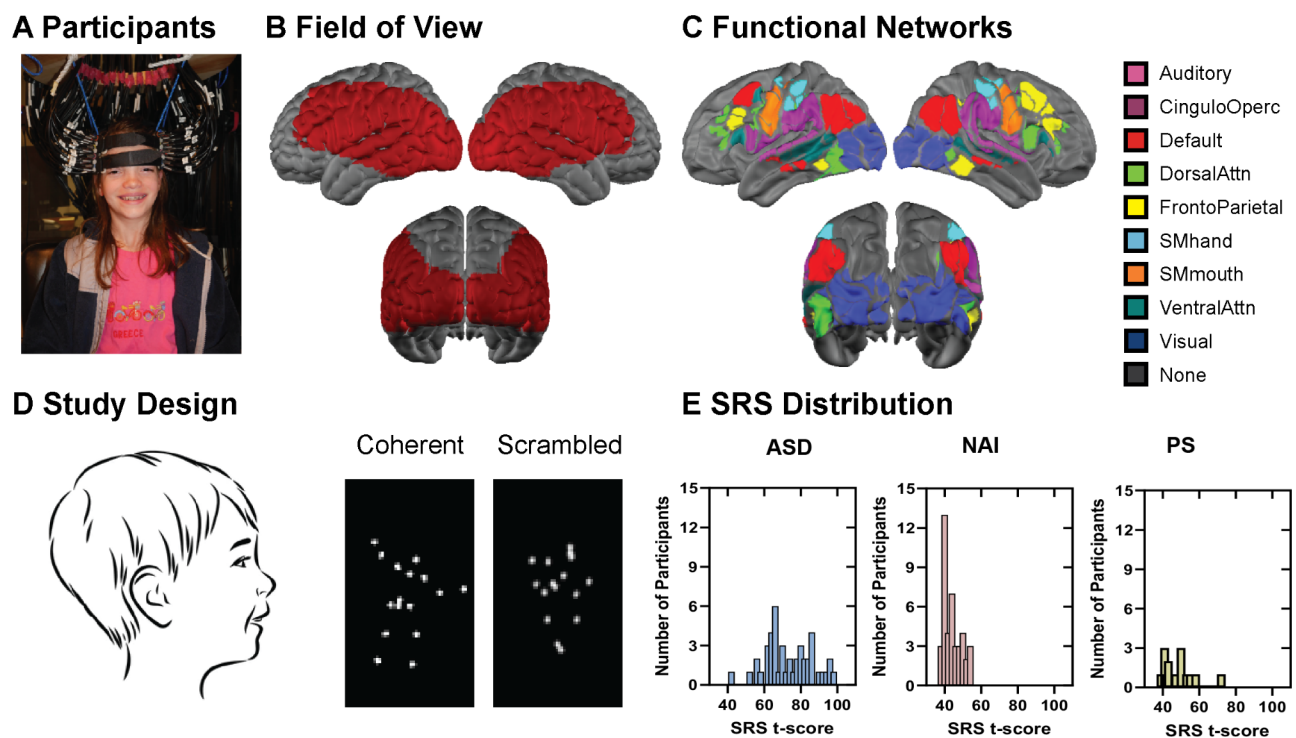


**Fig. 1** HD-DOT system and study Design. **A.** HD-DOT array on a school-age participant. **B.** The field of view of the HD-DOT system on the cortical surface. **C.** The DOT field of view, broken into parcels based on the Gordon parcellation, included 141 unique parcels and sampled auditory, cingulo-opercular (CinguloOperc), default mode, dorsal attention (DorsalAttn), frontal parietal (FrontoParietal), somatosensory hand (SMhand), somatosensory mouth (SMmouth), ventral attention (VentralAttn), visual, and no-assignment (None) functional networks. **D.** The study design of the biological motion perception experiment, participants passively viewed point-light displays of coherent biological and scrambled motion separately through a 20-inch (diagonal) LCD monitor. **E.** Distribution of the Social Responsiveness Scale-2 *t* scores for ASD, and NAI, and PS participants

by real-time readouts of quantitative assessments of optode-scalp coupling quality, including the mean light level and the coupling coefficient for each optode, and coupling variability for each optode. The imaging cap was placed comfortably on the head relative to anatomical landmarks of the left and right tragus andinion. The stimulus paradigm run was presented via Psychophysics Toolbox 3 (MATLAB, 2010b) using a 20-inch (diagonal) LCD screen 90 cm away from the participant's nation. The stimulus movie run consisted of alternating blocks of 24-second movies of point-light displays of coherent biological and scrambled motion (six movies of each type) - identical stimulus movies as previously used [26, 28]. No audio was presented during this task. Participants were instructed before each run to maintain attention on the stimulus and their attention to the stimulus was monitored throughout the session via web cams. Each stimulus run started and ended with a 30-second fixation period, for a total of 5 min and 48 s per run. Participants were requested to complete the biological motion perception task three times. Although some participants only completed the tasks twice, we obtained sufficient data from all participants included in the study for group analysis. Notably, there was no significant difference in the number of completed tasks between the NAI and ASD groups ( $t=0.0832$ ,  $p=0.9339$ ). Participants were additionally presented with auditory, visual, and moving-viewing tasks; however, these data are not included in this report.

#### Data Processing and image reconstruction

The HD-DOT data were processed using the NeuroDOT processing pipeline in MATLAB (<https://www.nitrc.org/projects/neurodot/>). Briefly, individual source-detector pair light-level measurements were converted into movies of relative hemodynamic changes at the voxel level through five steps: light-level measurement pre-processing, anatomical light modeling, image reconstruction, spectroscopy, and spatial normalization. The resultant data were movies of blood oxygenation level-dependent signals of relative changes in oxygenated hemoglobin (HbO) and deoxygenated hemoglobin (HbR). As we did not collect participant-specific MRI anatomy, following previous HD-DOT studies, we incorporated a standard MNI atlas-representative head model for image reconstruction [15, 19–23, 25], which we have previously shown provides mean image errors under 7 mm [14], as opposed to mean errors of 5 mm when using a participant specific head model [16]. As such, we expect errors due to using the atlas-based approach to be within inter-participant variability [59]. Herein, we focus on the HbO results due to its superior signal-to-noise ratio in comparison to HbR [15, 20, 60]. Details regarding these procedures have been previously published [14, 15] and are described in the supplementary methods.

#### Data quality assessment

To ensure data reliability, we assessed data quality using the following three metrics: (i) the pulse signal-to-noise ratio (SNR), (ii) the good measurement percentage, and (iii) the global variance of the temporal derivative (GVTD). The pulse SNR was calculated as the ratio of the integrated band-limited power at the pulse frequency (within a window of 0.5–2 Hz) to the median power in the same bandwidth immediately next to the pulse band. This metric assesses sensitivity of the measurement to vascular physiology, and therefore is an excellent measure of strong optical coupling of the system to the scalp. A threshold pulse SNR of 1 dB was employed to filter out runs with poor optode-scalp coupling [61]. The good measurement (GM) percentage was calculated as the percentage of measurements with a temporal standard deviation less than 7.5% [62]. To ensure consistent spatial coverage of the field of view, runs with less than 80% GM were excluded for further analysis. The GVTD metric, much like the DVARS (D referring to temporal derivative of time courses, VARS referring to root mean square variance over voxels) measure of fMRI, was calculated as the root mean square across the first temporal derivative of all first nearest neighbor measurements of both wavelengths [62]. The GVTD is a data-driven motion metric for fNIRS and HD-DOT and has been validated to outperform direct accelerometer measures and other motion correction methods [62]. Lower GVTD values correspond to HD-DOT maps with high spatial similarity against gold standard fMRI maps [62]. Here, we used GVTD to quantify the levels of motion and we removed data with high levels of motion using an empirical GVTD threshold of 0.1% [20, 61].

#### Biological motion data analysis

A general linear model was used to estimate within-participant beta values of coherent biological motion, scrambled motion, and their contrast (coherent > scrambled) in both HbO and HbR, using an HD-DOT-derived hemodynamic response function [63]. Mean beta maps for each participant were generated by averaging beta values from all runs that passed our stringent data quality and motion thresholding.

#### Statistical analysis

We tested for potential differences in age, VIQ, NVIQ, SRS, GM, and GVTD between groups with the Wilcoxon rank sum test. We used Fisher's exact test to test for differences in the proportion of females. While 12 PS participants passed data quality thresholds, the small sample size precluded meaningful statistical power. Thus, we excluded the PS participants from group level analyses. However, we included metrics of data quality and Social Responsiveness Scale (SRS) distribution analyses for the



PS group to ensure transparency and completeness and exclude from group level analysis. After stringent data quality thresholds ( $\text{SNR} > 1$  dB,  $\text{GM} > 80\%$ ) and matching NAI and ASD groups for mean GVTD, IQ, the presence of SRS measures, sex, and age, 21 NAI and 23 ASD participants were included in the analyses. Cluster-extent based thresholding was performed in SPM12 (Wellcome Trust Centre for Neuroimaging, London, UK) using the mean beta maps for each participant as input, cluster-extent-based thresholds ( $k$ ) calculated assuming a Gaussian random field [63], and a voxel-level  $p$ -value threshold ( $p < 0.0075$ ). In Kaiser et al., *PNAS*, 2010, the voxel-level  $p$ -value threshold was set at an uncorrected value of 0.0025 as they considered three separate conjunction analyses (i.e., state:  $\text{NAI} > \text{ASD}$  and  $\text{PS} > \text{ASD}$ , trait:  $\text{NAI} > \text{ASD}$  and  $\text{NAI} > \text{PS}$ , and compensatory:  $\text{PS} > \text{NAI}$  and  $\text{PS} > \text{ASD}$ ). Given that our final analysis did not use separate conjunction analysis, we applied a threshold for the voxelwise  $p = 0.0025 \times 3 = 0.0075$  to ensure robust control of multiple statistical comparisons. The residual images were used to estimate intrinsic smoothness for the contrast effects (i.e., coherent > scrambled). Two-sample  $t$ -tests compared task contrast effects within and across the NAI and ASD groups, with  $p < 0.0125$  for each tail with a false discovery rate (FDR) correction to control for multiple comparisons [64]. For the within-group statistics, we used paired  $t$ -tests. For the between group comparisons, we used two-sample  $t$ -tests. The selected thresholds were chosen to account for the two conditions/groups (coherent vs. scrambled or ASD vs. NAI) and two tails, leading to a threshold of  $0.05/4 = 0.0125$ . We used the WFU PickAtlas 3.0.5b [65] to identify anatomical reference naming for the given MNI coordinate locations for each surviving cluster. Regions of interest (ROI) surviving cluster correction were used for correlation analyses with the SRS  $t$ -scores. The mean contrast (coherent > scrambled) beta values within the corresponding clusters for each participant were correlated with the SRS  $t$ -score using Pearson correlations. Clusters with nominally significant correlations ( $p < 0.05$ ; FDR corrected) were further analyzed with hierarchical regression models for descriptive analyses.

As a secondary analysis, we used the Gordon cortical parcellation [66] to provide an unbiased spatial sampling for exploratory analyses of the relationship between BMP brain responses and SRS  $t$ -scores. The functionally defined Gordon parcellation provided a framework to couch our exploratory brain-wide analyses of brain-behavior relationships within functionally identified regions of interest. The intersection of each Gordon parcel with the HD-DOT field of view provided 141 parcels associated with nine functional networks (i.e., auditory, frontal-parietal, default mode, dorsal-attention, somatosensory hand, somatosensory mouth, ventral attention,

cingulo-opercular, and visual functional networks; Fig. 1C). Small parcels of size  $< 500 \text{ mm}^3$  were excluded from analyses. We averaged the beta contrast values within each parcel and calculated Pearson correlations as above. We ran descriptive analyses using hierarchical regression models for data in parcels passing a nominal significance level ( $p < 0.025$ ; FDR corrected) to generate hypotheses for future studies.

We used hierarchical linear regression analyses to test for confounding effects due to age, sex, cognitive function, and data quality metrics in the relationships between brain contrast and SRS  $t$ -score (IBM SPSS Statistics, Version 29.0). The hierarchical regression analysis allowed investigation of the relationships between brain contrast and SRS  $t$ -scores while accounting for associations of other variables of both interest (age, sex, cognitive scales) and non-interest (GVTD-assessed motion) with SRS scores. Reported relationships between contribution of brain activation differences and the SRS entail are thus estimated above and beyond these other factors." In each hierarchical regression analysis, the first model included participants' demographic information (i.e., age and sex) as predictor variables. The second model included Model 1 predictors and cognitive scores (i.e., NVIQ and VIQ). The third model added the motion (GVTD) and data quality (GM) variables with Model 2 predictors. The fourth model included Model 3 predictors and autism traits (i.e., SRS  $t$ -score). We checked the normality of the regression model residuals and visually inspected for violation of randomness and homoscedasticity with residual plots. Additionally, we checked the collinearity of variables with the variable inflation factors (VIF) and found that the VIF in all models was below five, the problematic threshold for collinearity.

## Results

### Behavioral/Demographic data

The final cohorts meeting full inclusion criteria were composed of 23 participants in the ASD group (SRS  $t$ -score =  $70.43 \pm 10.91$ , VIQ =  $100.61 \pm 14.10$ , and NVIQ =  $105.04 \pm 10.29$ ), 21 participants in the NAI group (SRS  $t$ -score =  $42.10 \pm 4.05$ , VIQ =  $106.05 \pm 9.83$ , and NVIQ =  $109.77 \pm 12.92$ ), and 12 participants in the PS group (SRS  $t$ -score =  $47.25 \pm 9.09$ , VIQ =  $107.58 \pm 12.10$ , and NVIQ =  $107.42 \pm 9.73$ ). The final NAI and ASD cohorts were matched in the proportion of females ( $p = 0.099$ ), age ( $z = -1.516$ ,  $p = 0.130$ ), and KBIT-2 verbal ( $t = 1.082$ ,  $p = 0.279$ ) and non-verbal scores ( $t = 1.754$ ,  $p = 0.079$ ). As expected, the SRS  $t$ -scores strongly differed with significantly higher  $t$ -scores for the ASD group than for the NAI group ( $z = 6.412$ ,  $p < 0.001$ ).

### HD-DOT feasibility and data quality evaluation

Data quality analyses revealed that 98.2% of participants ( $N=110$ ) had at least one experimental run with a pulse SNR greater than 1dB (Fig. 2Ai), and 89.2% of participants ( $N=100$ ) had at least one run with a GM percentage exceeding 80% (Fig. 2Bi). Additionally, 88.4% of participants ( $N=99$ ) had at least one run that satisfied both SNR greater than 1 dB and GM greater than 80% criteria. Further, 87.5% of participants ( $N=98$ ) had a run with a median GVTD lower than 0.1% (Fig. 2Ci). Importantly, there were no significant group differences in GM ( $z=0.724$ ,  $p=0.469$ ; Fig. 2Bii) or motion (GVTD;  $z=1.80$ ,  $p=0.07$ ; Fig. 2Cii) in the final cohorts.

### Within- and between- group brain activity

The maps of the  $t$ -tests (i.e.,  $t$ -maps) for the NAI group exhibited bilateral patterns of contrast as measured by HbO concentration changes (Fig. 3A). Specifically, cluster-corrected NAI group results showed implicated regions in the left inferior occipital gyrus (IOG), right middle occipital gyrus (MOG), bilateral inferior frontal gyrus (IFG), right superior temporal gyrus (STG), and right postcentral gyrus (PCG) (Fig. 3A and Table 2). In contrast, the ASD group (Fig. 3B) exhibited a strong contrast only in the right hemisphere, including the middle frontal gyrus (MFG), right MOG, middle temporal gyrus (MTG), and PCG. Complementary results are presented

for the HbR contrast in Supplementary Fig. 1 and Supplementary Table 1.

The contrast in brain activity between the NAI and ASD groups showed greater contrast in NAI than the ASD group in multiple regions (Fig. 3C). The cluster-corrected results revealed that the NAI group exhibited a significantly greater contrast than the ASD group in bilateral IFG, left lingual gyrus, left fusiform gyrus (FFG), left PCG, and right IOG (cluster-wise threshold  $p<0.0125$ ; Fig. 3C). The ASD group did not exhibit significantly greater contrast activity than NAI in any regions (Table 2).

### Relationship between brain function and SRS

To evaluate potential brain-behavior relationships, we correlated the parent-reported SRS  $t$ -scores with mean contrast magnitudes in the ten identified clusters within each group (those shown in Fig. 3A and B, and Table 2). These analyses revealed positive correlations between SRS  $t$ -score and cortical contrasts in the ASD group in five regions: right IFG ( $r=0.511$ ,  $p=0.013$ ), right STG ( $r=0.512$ ,  $p=0.013$ ), right MFG ( $r=0.527$ ,  $p=0.010$ ), right MOG ( $r=0.625$ ,  $p=0.001$ ), and right MTG ( $r=0.443$ ,  $p=0.034$ ). There were no significant correlations between contrast magnitudes and SRS  $t$ -score in the NAI group.

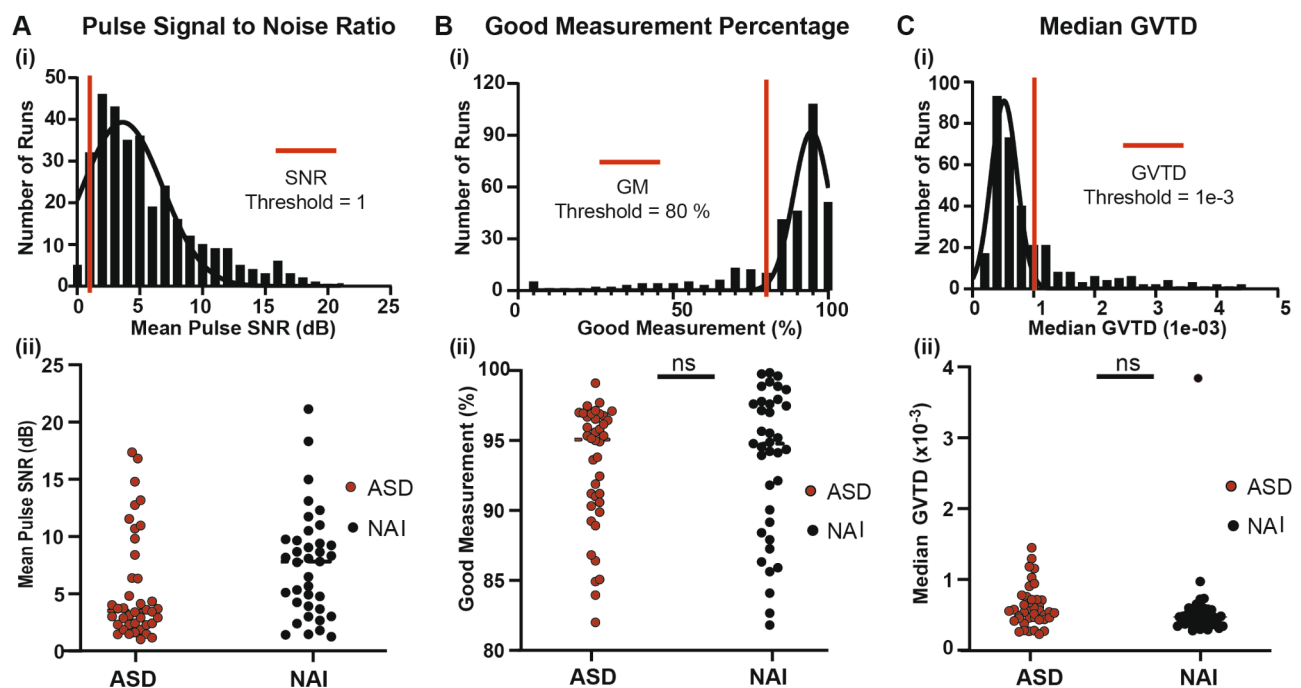


**Fig. 2** Data quality assessment. **A.** Distribution of mean signal-to-noise ratio in the pulse frequency band (i.e., 0.5–2 Hz) from (i) full samples (participant number = 112, 321 biological motion runs) and (ii) final samples (i.e., participant number = 44, NAI  $n=21$ , and ASD  $n=23$ ). **B.** Distribution of good measurement percentage of all measurements within 4 cm source-detector separation for (i) full and (ii) final sample. NAI and ASD groups did not significantly differ from each other ( $p=0.469$ ,  $z=0.724$ ). **C.** Distribution of post-censoring median GVTD (i) of all runs of all participants and (ii) final sample. In the final sample, there is no significant difference in median GVTD ( $p=0.07$ ,  $z=1.8$ ) between NAI and ASD cohorts

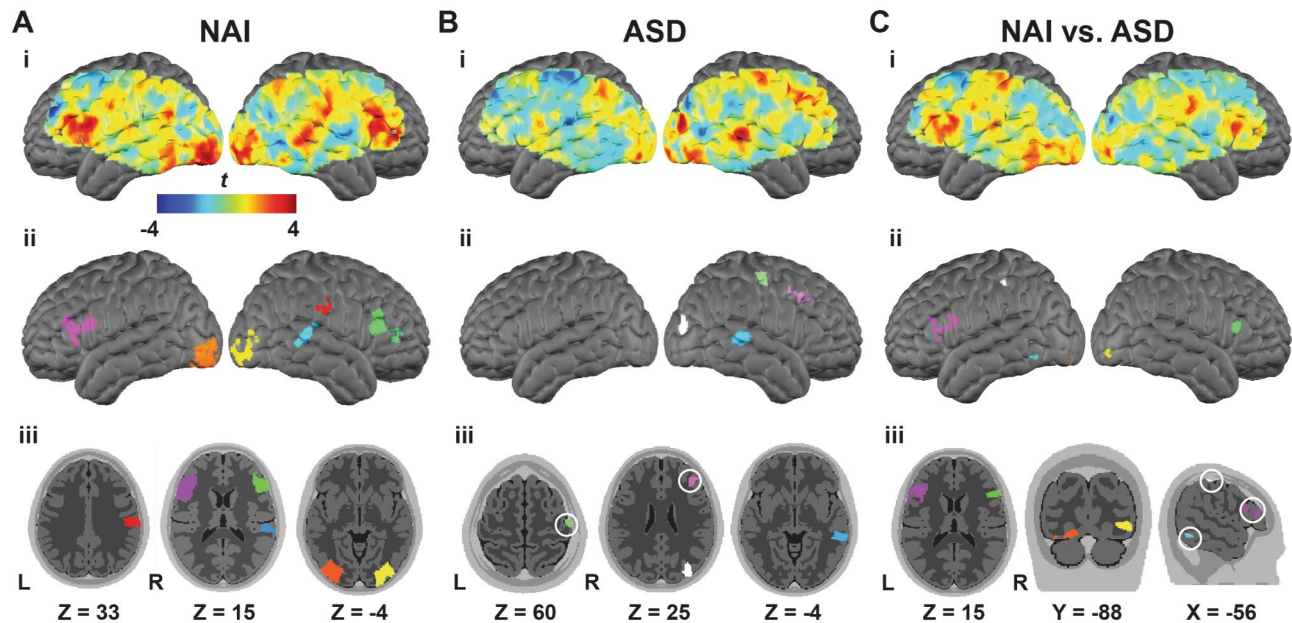


**Fig. 3** Within and between group contrast (coherent > scrambled biological motion) for HbO. **A(i)**. NAI children ( $n=21$ ) unthresholded  $t$ -map. Red regions indicate a greater response to coherent biological motion, while blue regions indicate a greater response to scrambled motion. Cluster correction revealed six regions of significant activity, visualized on the cortical **A(ii)** surface and within the **A(iii)** volume. **B(i)**. Autistic children ( $n=23$ ) unthresholded  $t$ -map. Cluster correction results in four significant regions of contrast activity, shown on the **B(ii)** cortical surface and **B(iii)** volumetric maps. **C(i)**. Welch-Satterthwaite corrected  $t$ -map showing NAI contrast greater than ASD. Red regions indicate greater NAI contrast activity ASD. Cluster correction revealed six significant regions visualized on the **C(ii)** surface and within the **C(iii)** volume. Cluster-corrected maps are thresholded at voxel-wise  $p < 0.0075$  and FDR-corrected at a cluster significance of  $p < 0.0125$

**Table 2** Anatomical regions of peak contrast activity for HbO

Contrast	BA	k (mm <sup>3</sup> )	T peak, mean	x (mm)	y (mm)	z (mm)
<b>NAI (coherent &gt; scrambled)</b>						
Inferior Occipital Gyrus (L)	18	18892	7.41, 3.53	-41	-99	-12
Middle Occipital Gyrus (R)	18	9328	4.76, 3.14	44	-92	-9
Inferior Frontal Gyrus (L)	46	8762	4.36, 3.01	-59	28	12
Inferior Frontal Gyrus (R)	46	6376	4.52, 3.08	56	28	23
Superior Temporal Gyrus (R)	22	3202	3.72, 2.90	73	-45	-1
Postcentral Gyrus (R)	2	2382	3.36, 2.80	64	-22	33
<b>ASD (coherent &gt; scrambled)</b>						
Middle Frontal Gyrus (R)	9	4906	3.80, 2.97	43	12	45
Middle Occipital Gyrus (R)	19	4506	5.47, 3.61	44	-92	20
Middle Temporal Gyrus (R)	22	4238	4.61, 3.43	61	-36	2
Postcentral Gyrus (R)	3	2097	3.33, 2.84	59	-17	57
<b>NAI v ASD (NAI &gt; ASD)</b>						
Inferior Frontal Gyrus (L)	45	5757	4.14, 2.92	-68	8	21
Lingual Gyrus (L)	18	1870	5.23, 2.80	-41	-100	-12
Fusiform Gyrus (L)	37	1607	3.63, 2.69	-72	-57	-9
Postcentral Gyrus (L)	2	1555	3.17, 2.76	-57	-32	59
Inferior Occipital Gyrus (R)	18	1369	3.87, 2.98	43	-92	-9
Inferior Frontal Gyrus (R)	45	1255	3.33, 2.83	59	24	14

\* MNI peak coordinates, corresponding extent cluster sizes (in mm<sup>3</sup>), and  $t$ -values of brain regions exhibiting significant contrast activity (coherent > scrambled). BA: Brodmann Area

**Brain-wide exploratory parcel-based analysis**

A brain-wide exploratory correlation analysis in Gordon parcels that intersected the HD-DOT field of view (Fig. 4) revealed eight significant parcels ( $p < 0.025$ ; Fig. 5). In the

NAI sample, contrast magnitudes in the left fusiform parcel exhibit a positive correlation ( $r=0.568$ ,  $p=0.007$ ) with SRS  $t$ -score. In the ASD group, the left angular gyrus was negatively correlated ( $r = -0.571$ ,  $p=0.004$ )



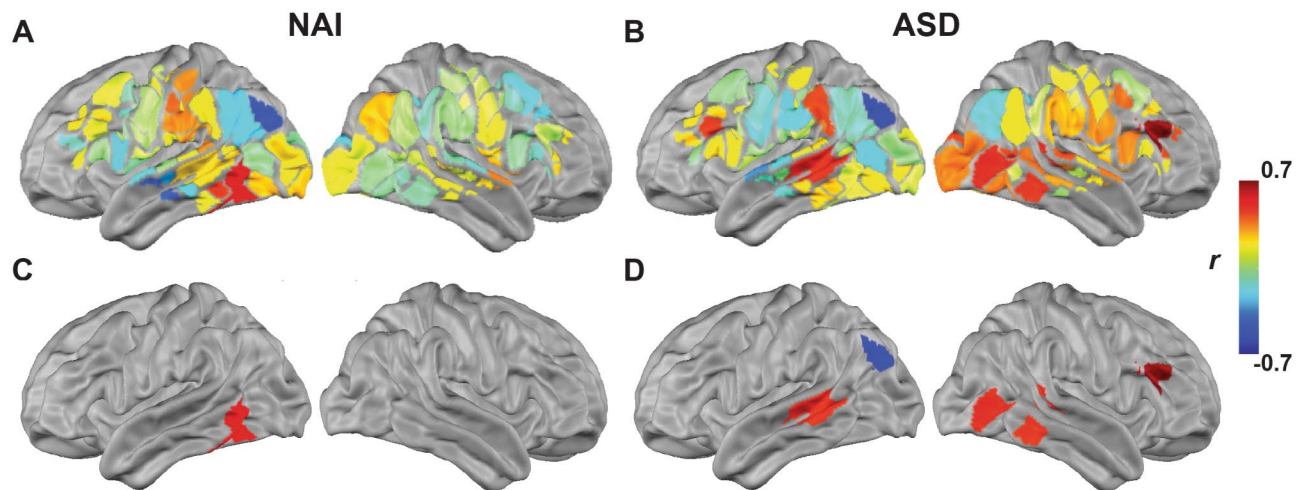


**Fig. 4** Parcel based correlation map between SRS  $t$ -score and beta contrast values. The maps depict brain-wide correlations across **A** 21 NAI and **B** 23 ASD participants. Positive correlations are represented in red, while negative correlations are shown in blue. Parcels with nominally significant correlations ( $p < 0.025$ ) are highlighted for both **C** NAI and **D** ASD groups

with SRS  $t$ -score, while other regions were positively correlated with SRS  $t$ -score, including the right dorsolateral prefrontal cortex ( $r=0.701$ ,  $p < 0.001$ , FDR adjusted  $p=0.008$ ), two parcels in the right STG ( $r=0.557$ ,  $p=0.006$ , and  $r=0.501$ ,  $p=0.015$ ), visual association ( $r=0.493$ ,  $p=0.017$ ), left MTG ( $r=0.475$ ,  $p=0.022$ ), and right MTG ( $r=0.473$ ,  $p=0.023$ ).

#### Hierarchical regression model analysis

To investigate how brain activity in specific ROI (as derived via either SPM clusters or Gordon parcels) relates to SRS given potential confounds of other variables, thirteen hierarchical linear regressions were conducted with four models of variables (i.e., demographic characteristics, cognitive scores, data quality and motion, and autism traits). The overall explained variance greatly improved in Model 4 when the SRS  $t$ -score was included as a predictor of the brain responses in all selected parcels and clusters in the ASD sample. Notably, in Model 4, the inclusion of the SRS  $t$ -score as a predictor led to a positive correlation between brain activity in specific regions of right STG, right MOG, right MFG, and left MTG. Conversely, a negative association was observed between the contrast in the left angular gyrus and SRS  $t$ -score. While Model 4 was improved after adding the SRS, age and IQ variables also contributed somewhat to the predicted brain activity in the right IFG, right MTG, and right dlPFC. Further, age, IQ, and GVTD variables showed moderate associations with parcel-specific brain activity in the right STG, right VAC, and left MTG in Models 1–3, although the impact was far less pronounced compared to the influence of SRS  $t$ -score in Model 4. Interestingly, no improvement was observed in explaining parcel-specific brain activity across models in

the NAI group. Detailed results are presented in Supplementary Tables 2–4.

#### Discussion

We aimed to establish the feasibility of HD-DOT for investigating brain function in autistic and non-autistic school-aged children and adolescents. Our results support the hypothesis that HD-DOT is feasible for assessing brain function in children during passive viewing of biological motion point-light displays, including autistic children. HD-DOT demonstrated robust performance across a cohort of 112 participants, each of whom completed a minimum of two tasks with good data quality (Fig. 2). While our final cohort sizes were smaller than planned due to data collection disruptions, the final sample size (ASD  $N=21$  and NAI  $N=23$ ) exceeds the median size (ASD  $N=17$ , NAI  $N=16$ ) observed in extant fMRI-based studies on biological motion in ASD [26–28, 48–51, 56, 67]. Second, our results for NAI implicate several regions previously reported to be associated with processing biological motion and social stimuli [27, 36, 48, 49, 67], including right STG, right PCG, right MOG, left IOG, and bilateral IFG (Fig. 3). Similarly, previous studies using fMRI in an NAI group reported corresponding patterns of brain activity in response to a similar task paradigm [28, 50, 56]. Third, we observed the ASD group exhibited significant contrasts in the right MOG, right MFG, right MTG, and right PCG. While the ASD group findings in the right hemisphere align with existing literature [28], we did not observe similar results in the left hemisphere where effects have been previously reported [28]. The disparity in the ASD activation patterns may be due to the heterogeneity of ASD presentation [42, 44].

Regarding group differences in brain contrast (NAI > ASD or ASD > NAI) to coherent vs. scrambled

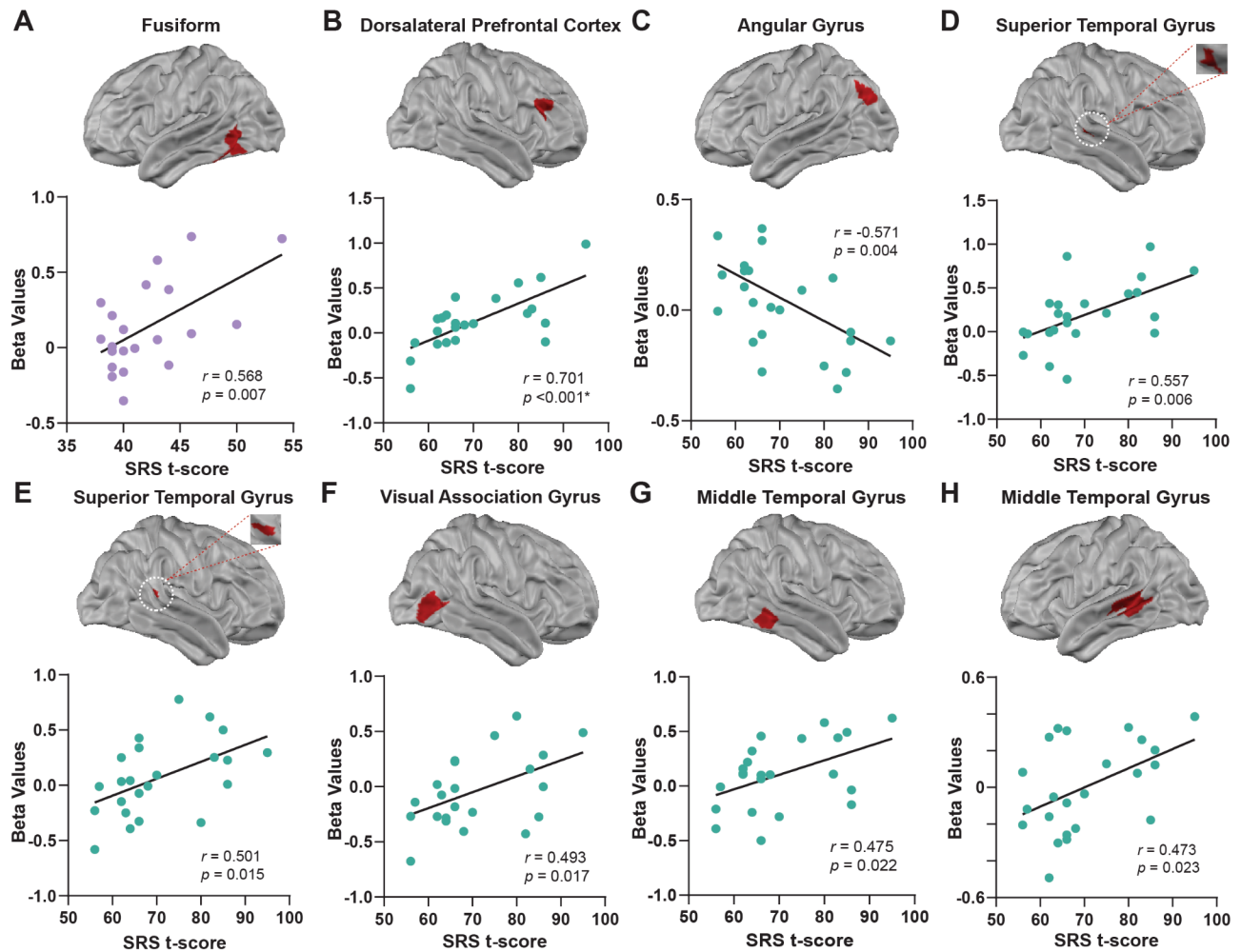


**Fig. 5** Parcels exhibiting correlation between SRS t-score and mean parcel beta contrast (coherent > scrambled). **A.** Left fusiform contrast positively correlated with SRS t-score in NAI group. **B.** Beta contrast in right dorsolateral prefrontal cortex positively correlated with SRS t-score in the ASD group. **C.** Negative correlation between SRS t-score and parcel-based brain activity in the angular gyrus in the ASD group. **D-H.** Positive correlations between brain contrast and SRS t-score in the ASD group

motion, we identified six distinct brain regions with greater contrast in the NAI group compared to the ASD group. First, we found that the bilateral IFG had greater contrast activity in the NAI group than the ASD group. Previous studies have also found less contrast activity in the IFG and overlapping/nearby regions, e.g., the ventrolateral prefrontal cortex, in response to biological motion in autistic children [26, 56, 68]. Previous fNIRS studies have suggested that autistic children have lower IFG activity during imitation tasks when compared to NAI [69]. Second, we found that the ASD cohort exhibited less contrast activity in the left lingual gyrus, left FFG, and right IOG compared to the NAI group. These regions are implicated in visual processing and object recognition, and studies of BMP have associated atypical activation in these regions to differences in processing socially relevant visual stimuli in autistic individuals [26–28]. Third, the NAI participants had greater contrast

than the ASD group in the left PCG. The PCG contains parts of the somatosensory system and is considered as part of the mirror-neuron system (MNS) [70, 71], which is involved in understanding, perceiving, and performing actions [70]. These findings indicate that NAI children may use the MNS for BMP processing to a larger degree than autistic children – a finding consistent with fMRI studies indicating that differences in MNS are associated with different facial and gesture imitation behaviors in autistic children [72–74]. Fourth, we observed that the right STG had greater contrast in the NAI group. However, inconsistent with previous fMRI studies [26, 28], we did not observe a statistically significant diminished contrast within the superior temporal sulcus in the ASD group compared to the NAI group. This inconsistency may be due to the heterogeneity in neural responses in ASD [42, 44]. Fifth, we did not observe any regions with statistically significant greater contrast activity in ASD

than in NAI. Indeed, only two out of 11 fMRI studies have reported cortical areas exhibiting greater contrast activity in an ASD group compared to an NAI group in response to a similar task paradigm [42]. To summarize, our study identified six distinct brain regions with greater contrast in NAI participants compared to the ASD group, and no regions with stronger contrast in the ASD group than the NAI group. Our findings, implicating specific cortical areas (i.e., bilateral IFG, left FFG, left PCG, and right IOG), strongly align with previous fMRI studies, thereby enhancing our overall understanding of the neural responses underlying BMP in ASD and NAI children.

Next, to investigate how the variability in brain function relates to variability in behavioral measures of autism traits, we correlated the brain contrast with SRS *t*-scores. Notably, positive correlations were observed in the right IFG, STG, MFG, MOG, and MTG across ASD participants. These results deviate from our hypothesis, as previous fMRI studies have reported negative correlations between SRS and brain contrast activity in regions linked to social processing [26, 28]. Intriguingly, an fMRI study using the identical experimental paradigm as this study also did not find any negative correlations between brain contrast and social responsiveness in the NAI group or carriers of heightened genetic likelihood for developing ASD [50]. In contrast, one fMRI study observed a similar positive correlation between a measure of autism trait severity (i.e., the Autism Quotient) and brain activity in ROI associated with BMP employing an identical experimental paradigm as the present study [56]. As demonstrated in a meta-analysis of BMP studies, variations in experimental paradigms, analysis methods, sample size, age range, cognitive ability, and heterogeneity in autism traits such as adaptive functioning may contribute to disparate results regarding neural correlates [42]. As an alternative secondary analysis, to provide an unbiased spatial sampling, we used the Gordon parcellation [66] to support a brain-wide exploratory analysis that implicated eight parcels (Figs. 4 and 5). The left angular gyrus parcel exhibited a negative correlation between the contrast response and SRS *t*-scores, aligning with prior studies [28]. The left angular gyrus plays a role in semantic processing, social cognition, and theory of mind [75, 76]. This negative correlation suggests that alterations in left angular gyrus response may contribute to social interaction and communication challenges observed in some autistic individuals. Additionally, our results revealed that the parcels located in the dlPFC, STG, VAC, and MTG exhibit positive correlations between brain contrast and SRS *t*-scores. These regions are associated with higher-order cognitive, visual, and social functioning [77–79]. Our results suggest that autistic children exhibiting stronger ASD traits display increased brain contrast activation in dlPFC, STG, VAC, and MTG. These findings

align with recent studies showing that while non-autistic individuals rely on specialized perceptual mechanisms for BMP [80, 81], autistic individuals may lack these mechanisms, or if present, they might be atypical development [40, 82]. Consequently, autistic individuals may employ higher-order cognitive and visual skills during perceiving or responding to BMP, possibly in the brain regions we identified as having positive correlations with autistic traits.

We found with the hierarchical regression analyses that the SRS *t*-scores more strongly related to variability in brain function than variables reflecting demographic information (e.g., age) and cognitive ability (e.g., VIQ and NVIQ), which is consistent with the existing literature [42, 83]. Age was a moderate predictor of variability in brain contrast in four ROIs in addition to SRS *t*-scores. Similarly, an activation likelihood estimation analysis of biological motion studies reported a significant main effect of age and determined age to be a moderator of the variance between studies [42]. Furthermore, previous studies found a relationship between IQ and biological motion perception in ASD [49, 83]. Likewise, we found that IQ measures were moderately related to region-specific brain contrasts in multiple regions. Taken together, while demographic and cognitive variables contributed somewhat to the explained variance in brain contrast, the SRS *t*-scores far more strongly predicted variability in the brain contrast in autistic children.

The methods herein combine the brain-specificity afforded by functional neuroimaging with the awake behavioral assessments that have generated some of the strongest predictive markers of likelihood and diagnosis of ASD [9, 84]. Quantifying characteristics of dimensional ASD traits with HD-DOT-measured brain function in early childhood in infants and toddlers will potentially inform outcome prediction and allow for measurement of changes in traits over time. Additionally, these methods will potentially enable monitoring of physiological responses to interventions, thereby advancing the search for underlying genetic and neurobiological mechanisms and aiding public health efforts to identify and support affected children to increase lifelong well-being. Further, given the open scanning environment, HD-DOT can be used to investigate direct within-room social communication and other differentiating core characteristics of autism. These HD-DOT methods are readily combined with eye tracking [84–86] and EEG [87, 88], two modalities usable in open settings and shown to be sensitive to behaviors and brain function associated with autism. HD-DOT may also be paired with computer vision-based approaches for digital phenotyping of body movements [89], imitation [89–91], and facial gestures [72]. Therefore, combining these methods may enable tremendous long-term potential to provide a better



understanding of developmental trajectories of the brain function underlying natural and differentiating behaviors and may thus provide profoundly improved predictive utility than current state-of-the-art behavioral assessments alone. Moreover, the expanding commercialization of emerging wearable HD-DOT systems will enable HD-DOT-based imaging throughout childhood development for those with a heightened likelihood for ASD and would provide a means to conduct brain function assessments (that may prove diagnostic) in natural settings, including within the clinic.

Overall, these findings highlight the reliability and effectiveness of HD-DOT to capture reliable neurological data and affirms its feasibility as a valuable tool for investigating brain function in autistic and non-autistic children. Given that HD-DOT is sensitive to responses to socially relevant stimuli in this age group, future studies may take advantage of the minimally-constraining environment of HD-DOT for evaluating brain function during more naturalistic tasks, such as movie viewing [92, 93], gesture imitation [73, 94], and direct dyadic social interaction [95, 96], even during live dyadic eye-to-eye contact [97]. Several fMRI, fNIRS, and HD-DOT studies indicate that, in contrast to strictly defined block design studies, naturalistic tasks more closely mimic real-life scenarios and interactions [98], leading to increased engagement, and greater ecological validity [92, 93, 98–102]. Furthermore, while imaging awake toddlers and infants has proven challenging, several fNIRS groups have successfully used optical methods throughout this young age range [54, 100, 103, 104]. Future work combining advanced optical imaging techniques, like HD-DOT, with naturalistic tasks will provide a unique opportunity to investigate neural mechanisms underlying development and social processing in ASD, including in infants and toddlers with a heightened likelihood for developing ASD [27].

### Limitations

Some limitations are important to consider. First, unlike fMRI, optical methods like fNIRS and HD-DOT are not sensitive to brain function in subcortical structures, such as those previously implicated in ASD-related differences, e.g., the amygdala and cerebellum [26, 42, 51, 68]. However, optical neuroimaging technology is sensitive to cortical brain function in multiple regions previously implicated in both task-based and task-free studies on ASD [13]. Importantly, HD-DOT allows for brain mapping in an open and naturalistic environment not possible with fMRI. Second, compared to traditional sparse fNIRS system, HD-DOT uses more sources and detectors, making it relatively bulkier, heavier, and more ergonomically challenging. However, HD-DOT provides better reliability, anatomical specificity, and imaging

quality than traditional sparse fNIRS systems [15, 22]. Importantly, HD-DOT technology is evolving rapidly, with multiple emerging research and commercial systems offering full-head fields of view with lightweight wearable designs that overcome the ergonomic limitations of the proof-of-principle HD-DOT system used in this study [25, 105, 106]. Third, while the eye gaze patterns were not quantitatively assessed in this study, participant gaze was consistently monitored, and participants were instructed to maintain their attention on the screen. Eye tracking, previously used to assess visual patterns and gaze positions [9, 107], can be naturally combined with optical methods for cross-modal investigations of brain function and eye gaze. Fourth, while point-light displays of biological motion are well-validated stimuli, a more naturalistic and ecologically valid task paradigm that drives social and emotional processing and requires direct engagement may provide a more powerful assay of visual-social processing. A more naturalistic task that requires behavioral responses would potentially enhance participant engagement with the stimulus, such as observing or imitating dynamic movements in movie clips [74]. Fifth, our study lacks enough female participants to assess sex-related differences or potential sex-by-diagnosis effects in BMP with meaningful statistical power. While the male-to-female ratio for ASD diagnosis is roughly 4:1 [108], recent investigations have suggested a more balanced sex ratio of the population having sub-clinical autism traits in light of under-diagnosis and exclusion of autistic females in research [109–111]. These investigations underscore the importance of evaluating and correcting for measurement bias related to sex, as well as identifying patterns of symptom presentation specific to each sex [112]. Larger studies with matched sex-ratios will be able to investigate the nuanced and complex effects of autosomal and sex-linked variability in brain function underlying behavioral autism traits [27, 108, 113]. Finally, our study lacked a sufficient sample size to include the proband siblings (PS) cohort in our primary analyses. We report the available aspects of the PS cohort data to ensure transparency and completeness. Additionally, given the previously demonstrated effects of genetic background on variability in autism-associated behavior and brain function [50, 84, 114, 115], future studies should continue to target PS participants.

### Conclusions

This study demonstrates the feasibility of HD-DOT for investigating brain activity in both autistic and non-autistic school-age children and establishes neural correlates with behavioral measures of social responsiveness. Our results show that both NAI and ASD groups tolerate HD-DOT scans well, exhibiting no differences in data quality or motion. Confirming results in fMRI studies,



we found that NAI children exhibit greater brain contrasts in regions linked to visual, motor, and social processing as compared to autistic children. Additionally, we established brain-behavior correlations between the brain contrast and SRS *t*-scores through both cluster-based and brain-wide parcel-based analyses. Overall, this study highlights the effectiveness of HD-DOT as promising tool for studying brain function in autistic children throughout childhood development in a naturalistic setting. Moreover, this research establishes neural correlates associated with biological motion processing and reveals the underlying relationships between these neural correlates and dimensional behavioral traits related to autism severity.

### Supplementary Information

The online version contains supplementary material available at <https://doi.org/10.1186/s13229-024-00614-4>.

Supplementary Material 1

### Acknowledgements

The authors would like to thank the children and families for participating in this study. We would also like to thank Dr. Kevin Pelphrey who provided the stimulus videos. We would also like to thank Anna Abbacchi and the Washington University Intellectual and Developmental Disabilities Research Center (WU-IDDRC) for participant characterization. All study procedures were approved by the Human Protections Office at Washington University School of Medicine Institutional Review Board, protocols #201705117 and #201101896. Written informed consent was obtained by all participants and parents (or guardians) of participants. The participant in the photo in Fig. 1, and her parent, consented for the image to be freely used in publications.

### Author contributions

Conceptualization: ATE, JNC, JPC, JRP. Data collection: AMS, AS, ATE, EF, MLS, PKM, SMR, KT, TBY, TGG. Formal analyses: AMS, ATE, DY, TGG, MDW, NNM. Methodology: ATE, JNC, JPC, JRP, NNM. Project administration: ATE. Resources: ATE, JPC. Software: ATE. Visualization: ATE, DY, TGG. Writing: AMS, ATE, DY, TGG. Funding acquisition: ATE. All authors read and approved the final manuscript.

### Funding

This work was supported by the National Institutes of Health (K01MH103594 and R01MH122751 to A.T.E.).

### Data availability

The datasets generated and analyzed during the current study, as well as the analysis codes, are available from the corresponding author upon request. All fully de-identified data will also be available on the NIMH data archive (NDA).

### Declarations

#### Ethics approval and consent to participate

All study procedures were approved by the Human Protections Office at Washington University School of Medicine Institutional Review Board, protocols #201705117 and #201101896. Written informed consent was obtained by all parents (or guardians) of participants and participants aged 18 and over.

#### Consent for publication

The girl in Fig. 1 was photographed and shared in the publication with written permission from her mother and her assent.

#### Competing interests

The authors declare no competing interests.

### Author details

- <sup>1</sup>Mallinckrodt Institute of Radiology, Washington University School of Medicine, 660 S. Euclid Ave, St. Louis, MO 63110, USA
- <sup>2</sup>Medical Education, Saint Louis University School of Medicine, St. Louis, MO 63104, USA
- <sup>3</sup>Department of Biomedical Engineering, Washington University School of Engineering, St. Louis, MO 63130, USA
- <sup>4</sup>Division of Biology and Biomedical Sciences, Washington University School of Medicine, St. Louis, MO 63110, USA
- <sup>5</sup>Department of Speech, Language, and Hearing Science, Purdue University, West Lafayette, IL 47907, USA
- <sup>6</sup>Department of Physics, Washington University School of Arts and Science, St. Louis, MO 63130, USA
- <sup>7</sup>Department of Neurology, University of California San Francisco, San Francisco, CA 94158, USA
- <sup>8</sup>University of Pittsburgh Medical Center, Western Psychiatric Hospital, Pittsburgh, PA 15213, USA
- <sup>9</sup>Evolvitycs, Parkville, MO 64152, USA
- <sup>10</sup>Doctor of Medicine Program, Washington University School of Medicine, St. Louis, MO 63110, USA
- <sup>11</sup>Department of Psychiatry, Washington University School of Medicine, St. Louis, MO 63110, USA
- <sup>12</sup>Department of Electrical and System Engineering, Washington University School of Engineering, St. Louis, MO 63112, USA
- <sup>13</sup>Department Imaging Sciences Engineering, Washington University School of Engineering, St. Louis, MO 63112, USA
- <sup>14</sup>Department of Psychiatry, Emory University School of Medicine, Atlanta, GA 30322, USA
- <sup>15</sup>Division of Behavioral and Mental Health, Children's Healthcare of Atlanta, Atlanta, GA 30329, USA

Received: 24 May 2024 / Accepted: 31 July 2024

Published online: 22 August 2024

### References

1. Association AP. Diagnostic and statistical manual of mental disorders (DSM-5). American Psychiatric Pub; 2013.
2. Maenner MJ, Warren Z, Williams AR, Amoakohene E, Bakian AV, Bilder DA, et al. Prevalence and characteristics of Autism Spectrum Disorder among children aged 8 years - Autism and Developmental Disabilities Monitoring Network, 11 sites, United States, 2020. *MMWR Surveill Summ*. 2023;72(2):1–14.
3. Sharpe DL. The Financial side of Autism: private and public costs. *sine loco: IntechOpen*; 2011.
4. Durkin MS, Maenner MJ, Meaney FJ, Levy SE, DiGiuseppi C, Nicholas JS, et al. Socioeconomic inequality in the prevalence of autism spectrum disorder: evidence from a U.S. cross-sectional study. *PLoS ONE*. 2010;5(7):e11551.
5. Lyall K, Croen L, Daniels J, Fallin MD, Ladd-Acosta C, Lee BK, et al. The changing epidemiology of Autism Spectrum disorders. *Annu Rev Public Health*. 2017;38:81–102.
6. Jacob A, Scott M, Falkmer M, Falkmer T. The costs and benefits of employing an adult with Autism Spectrum disorder: a systematic review. *PLoS ONE*. 2015;10(10):e0139896.
7. Estes A, Zwaigenbaum L, Gu H, St John T, Paterson S, Alison JT, et al. Behavioral, cognitive, and adaptive development in infants with autism spectrum disorder in the first 2 years of life. *J Neurodev Disord*. 2015;7(1):24.
8. Sharma SR, Gonda X, Tarazi FI. Autism spectrum disorder: classification, diagnosis and therapy. *Pharmacol Ther*. 2018;190:91–104.
9. Klin A, Lin DJ, Gorrindo P, Ramsay G, Jones W. Two-year-olds with autism orient to non-social contingencies rather than biological motion. *Nature*. 2009;459(7244):257–61.
10. Volkmar F, Chawarska K, Klin A. Autism spectrum disorders in infants and toddlers: An introduction. *Autism spectrum disorders in infants and toddlers: Diagnosis, assessment, and treatment*. 2008:1–22.
11. Everts R, Muri R, Leibundgut K, Siegwart V, Wiest R, Steinlin M. Fear and discomfort of children and adolescents during MRI: ethical consideration on research MRIs in children. *Pediatr Res*. 2022;91(4):720–3.
12. Li Y, Yu D. Variations of the functional Brain Network Efficiency in a young clinical sample within the Autism Spectrum: a fNIRS Investigation. *Front Physiol*. 2018;9:67.

13. Liu T, Liu X, Yi L, Zhu C, Markey PS, Pelowski M. Assessing autism at its social and developmental roots: a review of Autism Spectrum disorder studies using functional near-infrared spectroscopy. *NeuroImage*. 2019;185:955–67.
14. Ferradal SL, Eggebrecht AT, Hassanpour M, Snyder AZ, Culver JP. Atlas-based head modeling and spatial normalization for high-density diffuse optical tomography: in vivo validation against fMRI. *NeuroImage*. 2014;85(Pt 1):117–26.
15. Eggebrecht AT, Ferradal SL, Robichaux-Viehoever A, Hassanpour MS, Dehghani H, Snyder AZ, et al. Mapping distributed brain function and networks with diffuse optical tomography. *Nat Photonics*. 2014;8(6):448–54.
16. Eggebrecht AT, White BR, Ferradal SL, Chen C, Zhan Y, Snyder AZ, et al. A quantitative spatial comparison of high-density diffuse optical tomography and fMRI cortical mapping. *NeuroImage*. 2012;61(4):1120–8.
17. Ferradal SL, Liao SM, Eggebrecht AT, Shimony JS, Inder TE, Culver JP, et al. Functional imaging of the developing brain at the Bedside using diffuse Optical Tomography. *Cereb Cortex*. 2016;26(4):1558–68.
18. Zeff BW, White BR, Dehghani H, Schlaggar BL, Culver JP. Retinotopic mapping of adult human visual cortex with high-density diffuse optical tomography. Proceedings of the National Academy of Sciences. 2007;104(29):12169–74.
19. Habermehl C, Steinbrink J, Muller KR, Haufe S. Optimizing the regularization for image reconstruction of cerebral diffuse optical tomography. *J Biomed Opt*. 2014;19(9):96006.
20. Schroeder ML, Sherafati A, Ulbrich RL, Wheelock MD, Svoboda AM, Klein ED, et al. Mapping cortical activations underlying covert and overt language production using high-density diffuse optical tomography. *NeuroImage*. 2023;276:120190.
21. Sherafati A, Dwyer N, Bajracharya A, Hassanpour MS, Eggebrecht AT, Firszt JB et al. Prefrontal cortex supports speech perception in listeners with cochlear implants. *ELIFE*. 2022;11.
22. Fishell AK, Arbelaez AM, Valdes CP, Burns-Yocum TM, Sherafati A, Richter EJ et al. Portable, field-based neuroimaging using high-density diffuse optical tomography. *NeuroImage*. 2020;215.
23. Tripathy K, Fogarty M, Svoboda AM, Schroeder ML, Rafferty SM, Richter EJ, et al. Mapping brain function in adults and young children during naturalistic viewing with high-density diffuse optical tomography. *Hum Brain Mapp*. 2024;45(7):e26684.
24. Ferradal SL, Liao S, Eggebrecht AT, Shimony JS, Inder TE, Culver JP, et al. Functional imaging of the developing brain at the Bedside using diffuse Optical Tomography. *Cereb Cortex*. 2016;26(4):1558–68.
25. Uchitel J, Blanco B, Collins-Jones L, Edwards A, Porter E, Pammenter K, et al. Cot-side imaging of functional connectivity in the developing brain during sleep using wearable high-density diffuse optical tomography. *NeuroImage*. 2023;265:119784.
26. Kaiser MD, Hudac CM, Shultz S, Lee SM, Cheung C, Berken AM, et al. Neural signatures of autism. *Proc Natl Acad Sci U S A*. 2010;107(49):21223–8.
27. Björnsdóttir M, Wang N, Pelphrey K, Kaiser MD. Evaluation of Quantified Social Perception Circuit Activity as a neurobiological marker of Autism Spectrum Disorder. *JAMA Psychiatry*. 2016;73(6):614–21.
28. Yang YJ, Sukhodolsky DG, Lei J, Dayan E, Pelphrey KA, Ventola P. Distinct neural bases of disruptive behavior and autism symptom severity in boys with autism spectrum disorder. *J Neurodev Disord*. 2017;9:1.
29. Fujioka T, Inohara K, Okamoto Y, Masuya Y, Ishitobi M, Saito DN et al. Gaze-finder as a clinical supplementary tool for discriminating between autism spectrum disorder and typical development in male adolescents and adults. *Mol Autism*. 2016;7.
30. Krüger B, Kaletsch M, Pilgramm S, Schwippert SS, Hennig J, Stark R, et al. Perceived intensity of emotional point-light displays is reduced in subjects with ASD. *J Autism Dev Disord*. 2018;48(1):1–11.
31. Fujisawa TX, Tanaka S, Saito DN, Kosaka H, Tomoda A. Visual attention for social information and salivary oxytocin levels in preschool children with autism spectrum disorders: an eye-tracking study. *Front Neurosci*. 2014;8:295.
32. Johansson G. Visual-perception of Biological Motion and a model for its analysis. *Percept Psychophys*. 1973;14(2):201–11.
33. Fox R, McDaniel C. The perception of Biological Motion by Human infants. *Science*. 1982;218(4571):486–7.
34. Oram MW, Perrett DI. Integration of form and motion in the anterior superior temporal polysensory area (STPa) of the macaque monkey. *J Neurophysiol*. 1996;76(1):109–29.
35. Vallortigara G, Regolin L, Marconato F. Visually inexperienced chicks exhibit spontaneous preference for biological motion patterns. *PLoS Biol*. 2005;3(7):e208.
36. Johnson MH. Biological motion: a perceptual life detector? *Curr Biol*. 2006;16(10):R376–7.
37. Tian J, Yang F, Wang Y, Wang L, Wang N, Jiang Y, et al. Atypical biological motion perception in children with attention deficit hyperactivity disorder: dissociating the roles of local motion and global configuration Processing. *eLife Sciences Publications, Ltd*; 2023.
38. Sifre R, Olson L, Gillespie S, Klin A, Jones W, Shultz S. A longitudinal investigation of preferential attention to Biological Motion in 2- to 24-Month-Old infants. *Sci Rep*. 2018;8(1):2527.
39. Simion F, Regolin L, Bulf H. A predisposition for biological motion in the newborn baby. *Proc Natl Acad Sci U S A*. 2008;105(2):809–13.
40. Klin A, Jones W. Altered face scanning and impaired recognition of biological motion in a 15-month-old infant with autism. *Dev Sci*. 2008;11(1):40–6.
41. Di Giorgio E, Frasnelli E, Rosa Salva O, Luisa Scattoni M, Puopolo M, Tosoni D, et al. Difference in Visual Social predispositions between newborns at Low- and high-risk for Autism. *Sci Rep*. 2016;6(1):26395.
42. Todorova GK, Hatton REM, Pollick FE. Biological motion perception in autism spectrum disorder: a meta-analysis. *Mol Autism*. 2019;10:49.
43. Foglia V, Siddiqui H, Khan Z, Liang S, Rutherford MD. Distinct Biological Motion Perception in Autism Spectrum disorder: a Meta-analysis. *J Autism Dev Disord*. 2022;52(11):4843–60.
44. Federici A, Parma V, Vicovaro M, Radassao L, Casartelli L, Ronconi L. Anomalous perception of Biological Motion in Autism: a conceptual review and Meta-analysis. *Sci Rep*. 2020;10(1):4576.
45. Wang L, Wang B, Wu C, Wang J, Sun M. Autism spectrum disorder: neurodevelopmental risk factors, Biological mechanism, and Precision Therapy. *Int J Mol Sci*. 2023;24(3).
46. Ortu D, Vaidya M. The challenges of integrating behavioral and neural data: bridging and Breaking Boundaries across Levels of Analysis. *Behav Anal*. 2017;40(1):209–24.
47. Uddin LQ, Supekar K, Lynch CJ, Khouzam A, Phillips J, Feinstein C, et al. Saliency network-based classification and prediction of symptom severity in children with autism. *JAMA Psychiatry*. 2013;70(8):869–79.
48. Alaerts K, Swinnen SP, Wenderoth N. Neural processing of biological motion in autism: an investigation of brain activity and effective connectivity. *Sci Rep*. 2017;7(1):5612.
49. Koldewyn K, Whitney D, Rivera SM. Neural correlates of coherent and biological motion perception in autism. *Dev Sci*. 2011;14(5):1075–88.
50. Eggebrecht AT, Dworetzky A, Hawks Z, Coalson R, Adeyemo B, Davis S, et al. Brain function distinguishes female carriers and non-carriers of familial risk for autism. *Mol Autism*. 2020;11(1):82.
51. Jack A, Keifer CM, Pelphrey KA. Cerebellar contributions to biological motion perception in autism and typical development. *Hum Brain Mapp*. 2017;38(4):1914–32.
52. Stogiannos N, Pavlopoulou G, Papadopoulou C, Walsh G, Potts B, Moqbel S, et al. Strategies to improve the magnetic resonance imaging experience for autistic individuals: a cross-sectional study exploring parents and carers' experiences. *BMC Health Serv Res*. 2023;23(1):1375.
53. Wheelock MD, Culver JP, Eggebrecht AT. High-density diffuse optical tomography for imaging human brain function. *Rev Sci Instrum*. 2019;90(5):051101.
54. Fox SE, Wagner JB, Shrock CL, Tager-Flusberg H, Nelson CA. Neural processing of facial identity and emotion in infants at high-risk for autism spectrum disorders. *Front Hum Neurosci*. 2013;7:89.
55. Bortfeld H, Wruck E, Boas DA. Assessing infants' cortical response to speech using near-infrared spectroscopy. *NeuroImage*. 2007;34(1):407–15.
56. Puglia MH, Morris JP. Neural response to Biological motion in healthy adults varies as a function of autistic-like traits. *Front Neurosci*. 2017;11:404.
57. Kauffman JM, Weaver SJ, Weaver A. Age and intelligence as correlates of perceived family relationships of underachievers. *Psychol Rep*. 1971;28(2):522.
58. Constantino JN, Gruber CP. Social responsiveness scale: SRS-2. Second edition ed. Torrance, California: Western Psychological Services; 2012. v, 106 pages p.
59. Fedorenko E, Hsieh PJ, Nieto-Castanon A, Whitfield-Gabrieli S, Kanwisher N. New method for fMRI investigations of language: defining ROIs functionally in individual subjects. *J Neurophysiol*. 2010;104(2):1177–94.
60. Yucel MA, Luhmann AV, Scholkmann F, Gervain J, Dan I, Ayaz H, et al. Best practices for fNIRS publications. *Neurophotonics*. 2021;8(1):012101.
61. Fishell AK, Arbelaez AM, Valdes CP, Burns-Yocum TM, Sherafati A, Richter EJ et al. Portable, field-based neuroimaging using high-density diffuse optical tomography. *NeuroImage*. 2020;116541.
62. Sherafati A, Snyder AZ, Eggebrecht AT, Bergonzi KM, Burns-Yocum TM, Lugar HM et al. Global motion detection and censoring in high-density diffuse optical tomography. *Hum Brain Mapp*. 2020.

63. Hassanpour MS, White BR, Eggebrecht AT, Ferradal SL, Snyder AZ, Culver JP. Statistical analysis of high density diffuse optical tomography. *NeuroImage*. 2014;85(Pt 1):104–16.
64. Benjamini Y, Hochberg Y. Controlling the false Discovery Rate - a practical and powerful Approach to multiple testing. *J R Stat Soc B*. 1995;57(1):289–300.
65. Maldjian JA, Laurienti PJ, Kraft RA, Burdette JH. An automated method for neuroanatomic and cytoarchitectonic atlas-based interrogation of fMRI data sets. *NeuroImage*. 2003;19(3):1233–9.
66. Gordon EM, Laumann TO, Adeyemo B, Huckins JF, Kelley WM, Petersen SE. Generation and evaluation of a cortical area parcellation from resting-state correlations. *Cereb Cortex*. 2016;26(1):288–303.
67. Freitag CM, Konrad C, Haberlen M, Kleser C, von Gontard A, Reith W, et al. Perception of biological motion in autism spectrum disorders. *Neuropsychologia*. 2008;46(5):1480–94.
68. Peng Z, Chen Y, Jin L, Han H, Dong C, Guo Y, et al. Social brain dysfunctionality in individuals with autism spectrum disorder and their first-degree relatives: an activation likelihood estimation meta-analysis. *Psychiatry Res Neuroimaging*. 2020;298:111063.
69. Mori K, Toda Y, Ito H, Mori T, Mori K, Goji A, et al. Neuroimaging in autism spectrum disorders: 1H-MRS and NIRS study. *J Med Invest*. 2015;62(1–2):29–36.
70. Lamm C, Fischer MH, Decety J. Predicting the actions of others taps into one's own somatosensory representations—a functional MRI study. *Neuropsychologia*. 2007;45(11):2480–91.
71. Wu H, Tang H, Ge Y, Yang S, Mai X, Luo YJ, et al. Object words modulate the activity of the mirror neuron system during action imitation. *Brain Behav*. 2017;7(11):e00840.
72. Dapretto M, Davies MS, Pfeifer JH, Scott AA, Sigman M, Bookheimer SY, et al. Understanding emotions in others: mirror neuron dysfunction in children with autism spectrum disorders. *Nat Neurosci*. 2006;9(1):28–30.
73. Mostofsky SH, Dubey P, Jerath VK, Jansiewicz EM, Goldberg MC, Denckla MB. Developmental dyspraxia is not limited to imitation in children with autism spectrum disorders. *J Int Neuropsychol Soc*. 2006;12(3):314–26.
74. Tunçgenç B, Pacheco C, Rochowiak R, Nicholas R, Rengarajan S, Zou E, et al. Computerized Assessment of Motor Imitation as a scalable method for distinguishing children with autism. *Biol Psychiatr Cogn N*. 2021;6(3):321–8.
75. Kuhnke P, Chapman CA, Cheung VKM, Turker S, Graessner A, Martin S, et al. The role of the angular gyrus in semantic cognition: a synthesis of five functional neuroimaging studies. *Brain Struct Funct*. 2023;228(1):273–91.
76. Binder JR, Desai RH, Graves WW, Conant LL. Where is the Semantic System? A critical review and Meta-analysis of 120 functional neuroimaging studies. *Cereb Cortex*. 2009;19(12):2767–96.
77. Xiaoming J. Prefrontal Cortex: role in Language Communication during Social Interaction. In: Ana S, Branislav F, editors. *Prefrontal Cortex*. Rijeka: IntechOpen; 2018. Ch. 4.
78. Bigler ED, Mortensen S, Neeley ES, Ozonoff S, Krasny L, Johnson M, et al. Superior temporal gyrus, language function, and autism. *Dev Neuropsychol*. 2007;31(2):217–38.
79. Davey J, Thompson HE, Hallam G, Karapanagiotidis T, Murphy C, De Caso I, et al. Exploring the role of the posterior middle temporal gyrus in semantic cognition: integration of anterior temporal lobe with executive processes. *NeuroImage*. 2016;137:165–77.
80. Annaz D, Remington A, Milne E, Coleman M, Campbell R, Thomas MS, et al. Development of motion processing in children with autism. *Dev Sci*. 2010;13(6):826–38.
81. Nackaerts E, Wagemans J, Helsen W, Swinnen SP, Wenderoth N, Alaerts K. Recognizing biological motion and emotions from point-light displays in autism spectrum disorders. *PLoS ONE*. 2012;7(9):e44473.
82. Blake R, Turner LM, Smoski MJ, Pozdol SL, Stone WL. Visual recognition of biological motion is impaired in children with autism. *Psychol Sci*. 2003;14(2):151–7.
83. Rutherford MD, Troje NF. IQ predicts biological motion perception in autism spectrum disorders. *J Autism Dev Disord*. 2012;42(4):557–65.
84. Constantino JN, Kennon-McGill S, Weichselbaum C, Marrus N, Haider A, Glowinski AL, et al. Infant viewing of social scenes is under genetic control and is atypical in autism. *Nature*. 2017;547(7663):340–.
85. Klin A, Jones W, Schultz R, Volkmar F, Cohen D. Visual fixation patterns during viewing of naturalistic social situations as predictors of social competence in individuals with autism. *Arch Gen Psychiatr*. 2002;59(9):809–16.
86. Chang Z, Di Martino JM, Aiello R, Baker J, Carpenter K, Compton S, et al. Computational methods to measure patterns of Gaze in Toddlers with Autism Spectrum Disorder. *JAMA Pediatr*. 2021;175(8):827–36.
87. Marco EJ, Hinkley LBN, Hill SS, Nagarajan SS. Sensory processing in autism: a review of neurophysiologic findings. *Pediatr Res*. 2011;69(5 Pt 2):R48–54.
88. Yen CH, Lin CL, Chiang MC. Exploring the frontiers of neuroimaging: a review of recent advances in understanding Brain Functioning and disorders. *Life-Basel*. 2023;13:7.
89. Chaminade T, Meltzoff AN, Decety J. An fMRI study of imitation: action representation and body schema. *Neuropsychologia*. 2005;43(1):115–27.
90. Williams JHG, Whiten A, Suddendorf T, Perrett DI. Imitation, mirror neurons and autism. *Neurosci Biobehav R*. 2001;25(4):287–95.
91. Tunçgenç B, Pacheco C, Rochowiak R, Nicholas R, Rengarajan S, Zou E, et al. Computerized Assessment of Motor Imitation as a scalable method for distinguishing children with autism. *Biol Psychiatry Cogn Neurosci Neuroimaging*. 2021;6(3):321–8.
92. Bartels A, Zeki S. Functional brain mapping during free viewing of natural scenes. *Hum Brain Mapp*. 2004;21(2):75–85.
93. Fishell AK, Burns-Yocum TM, Bergonzi KM, Eggebrecht AT, Culver JP. Mapping brain function during naturalistic viewing using high-density diffuse optical tomography. *Sci Rep*. 2019;9(1):11115.
94. Nemani A, Yucel MA, Kruger U, Gee DW, Cooper C, Schwaizberg SD, et al. Assessing bimanual motor skills with optical neuroimaging. *Sci Adv*. 2018;4(10):eaat3807.
95. Suda M, Takei Y, Aoyama Y, Narita K, Sakurai N, Fukuda M, et al. Autistic traits and brain activation during face-to-face conversations in typically developed adults. *PLoS ONE*. 2011;6(5):e20021.
96. Kelley MS, Noah JA, Zhang X, Scassellati B, Hirsch J. Comparison of human Social Brain Activity during Eye-Contact with another human and a Humanoid Robot. *Front Robot Ai*. 2021;7.
97. Hirsch J, Zhang X, Noah JA, Dravida S, Naples A, Tiede M, et al. Neural correlates of eye contact and social function in autism spectrum disorder. *PLoS ONE*. 2022;17(11):e0265798.
98. Lahnakoski JM, Glerean E, Salmi J, Jaaskelainen IP, Sams M, Hari R, et al. Naturalistic FMRI mapping reveals superior temporal sulcus as the hub for the distributed brain network for social perception. *Front Hum Neurosci*. 2012;6:233.
99. Greene DJ, Koller JM, Hampton JM, Wesevich V, Van AN, Nguyen AL, et al. Behavioral interventions for reducing head motion during MRI scans in children. *NeuroImage*. 2018;171:234–45.
100. Lloyd-Fox S, Blasi A, Volein A, Everdell N, Ellwell CE, Johnson MH. Social perception in infancy: a near infrared spectroscopy study. *Child Dev*. 2009;80(4):986–99.
101. Vanderwal T, Kelly C, Eilbott J, Mayes LC, Castellanos FX. Inscapes: a movie paradigm to improve compliance in functional magnetic resonance imaging. *NeuroImage*. 2015;122:222–32.
102. Pollonini L, Bortfeld H, Oghalai JS. PHOEBE: a method for real time mapping of optodes-scalp coupling in functional near-infrared spectroscopy. *Biomed Opt Express*. 2016;7(12):5104–19.
103. Kikuchi M, Yoshimura Y, Shitamichi K, Ueno S, Hiraishi H, Munesue T, et al. Anterior prefrontal hemodynamic connectivity in conscious 3- to 7-year-old children with typical development and autism spectrum disorder. *PLoS ONE*. 2013;8(2):e56087.
104. Franceschini MA, Thaker S, Themelis G, Krishnamoorthy KK, Bortfeld H, Diamond SG, et al. Assessment of infant brain development with frequency-domain near-infrared spectroscopy. *Pediatr Res*. 2007;61(5 Pt 1):546–51.
105. Vidal-Rosas EE, Zhao H, Nixon-Hill RW, Smith G, Dunne L, Powell S, et al. Evaluating a new generation of wearable high-density diffuse optical tomography technology via retinotopic mapping of the adult visual cortex. *Neurophotonics*. 2021;8(2):025002.
106. Frijia EM, Billing A, Lloyd-Fox S, Vidal Rosas E, Collins-Jones L, Crespo-Llado MM, et al. Functional imaging of the developing brain with wearable high-density diffuse optical tomography: a new benchmark for infant neuroimaging outside the scanner environment. *NeuroImage*. 2021;225:117490.
107. Pua EPK, Bowden SC, Seal ML. Autism spectrum disorders: neuroimaging findings from systematic reviews. *Res Autism Spectr Disorders*. 2017;34:28–33.
108. Zhang Y, Li N, Li C, Zhang Z, Teng H, Wang Y, et al. Genetic evidence of gender difference in autism spectrum disorder supports the female-protective effect. *Transl Psychiatry*. 2020;10(1):4.
109. Lai MC, Szatmari P. Sex and gender impacts on the behavioural presentation and recognition of autism. *Curr Opin Psychiatry*. 2020;33(2):117–23.
110. Lockwood Estrin G, Milner V, Spain D, Happe F, Colvert E. Barriers to Autism Spectrum Disorder diagnosis for Young women and girls: a systematic review. *Rev J Autism Dev Disord*. 2021;8(4):454–70.

111. Nordahl CW. Why do we need sex-balanced studies of autism? *Autism Res.* 2023;16(9):1662–9.
112. Burrows CA, Grzadzinski RL, Donovan K, Stallworthy IC, Rutsohn J, St John T, et al. A Data-Driven Approach in an unbiased sample reveals equivalent sex ratio of Autism Spectrum Disorder-Associated impairment in early childhood. *Biol Psychiatry.* 2022;92(8):654–62.
113. Ferri SL, Abel T, Brodtkin ES. Sex differences in Autism Spectrum Disorder: a review. *Curr Psychiatry Rep.* 2018;20(2):9.
114. Girault JB, Donovan K, Hawks Z, Talovic M, Forsen E, Elison JT, et al. Brain imaging markers of inherited liability for autism implicate infant visual regions and pathways. *Am J Psychiatry.* 2022;179(8):573–85.
115. Ozonoff S, Young GS, Bradshaw J, Charman T, Chawarska K, Iverson JM et al. Familial Recurrence of Autism: Updates From the Baby Siblings Research Consortium. *Pediatrics.* 2024.

### **Publisher's Note**

Springer Nature remains neutral with regard to jurisdictional claims in published maps and institutional affiliations.